Sleep Research Society®

Article Navigation

Sleep stage dynamics in neocortex and hippocampus FREE

Ernesto Durán, Carlos N Oyanedel, Niels Niethard, Marion Inostroza, Jan Born

Sleep, Volume 41, Issue 6, June 2018, zsy060, https://doi.org/10.1093/sleep/zsy060
Published: 16 April 2018 **Article history ▾**

PDF Split View Cite Permissions Share ▼

Abstract

Mammalian sleep comprises the stages of slow-wave sleep (SWS) and rapid eye movement (REM) sleep. Additionally, a transition state is often discriminated which in rodents is termed intermediate stage (IS). Although these sleep stages are thought of as unitary phenomena affecting the whole brain in a congruent fashion, recent findings have suggested that sleep stages can also appear locally restricted to specific networks and regions. Here, we compared in rats sleep stages and their transitions between neocortex and hippocampus. We simultaneously recorded the electroencephalogram (EEG) from skull electrodes over frontal and parietal cortex and the local field potential (LFP) from the medial prefrontal cortex and dorsal hippocampus. Results indicate a high congruence in the occurrence of sleep and SWS (>96.5%) at the different recording sites. Congruence was lower for REM sleep (>87%) and lowest for IS (<36.5%). Incongruences occurring at sleep stage transitions were most pronounced for REM sleep which in 36.6 per cent of all epochs started earlier in hippocampal LFP recordings than in the other recordings, with an average interval of 17.2 ± 1.1 s between REM onset in the hippocampal LFP and the parietal EEG ($p < 0.001$). Earlier REM onset in the hippocampus was paralleled by a decrease in muscle tone, another hallmark of REM sleep. These findings indicate a region-specific regulation of REM sleep which has clear implications not only for our understanding of the organization of sleep, but possibly also for the functions, e.g. in memory formation, that have been associated with REM sleep.

slow-wave sleep, intermediate stage, REM sleep, prefrontal cortex, hippocampus, theta activity, muscle atonia

Statement of Significance

Sleep in mammals comprises the core sleep stages of slow-wave sleep (SWS) and rapid eye movement (REM) sleep which are thought of as unitary phenomena expressing themselves in a coherent way throughout the brain. We compared the occurrence of sleep and sleep stages in electroencephalogram recordings of cortical activity and local field potential recordings from prefrontal cortex and hippocampus. Although SWS congruently occurred in signals covering neocortical and hippocampal activity, REM sleep often started substantially earlier in the hippocampus than in neocortical networks. The findings indicate a region-specific regulation of REM sleep with implications for the functions commonly attributed to this stage.

Introduction

Classically, sleep and its composing sleep stages have been thought of as homogenous states that capture the whole organism, or at least the whole

brain. Based on such concept, sleep was defined using behavioral criteria, such as physical quiescence and increased arousal thresholds. The most widely accepted approach to characterize sleep is polysomnography which includes the simultaneous recording of electroencephalographic (EEG) and electromyographic (EMG) recordings and, additionally in humans, electrooculographic recordings [1, 2]. These signals allow us to differentiate in mammals the two principal sleep stages of slow-wave sleep (SWS) and rapid eye movement (REM) sleep [3, 4]. Additionally, in rodents and cats, a transition state between SWS and REM sleep can be discriminated which is called intermediate stage (IS) [5–7]. Although all these sleep stages are considered as global phenomena, in recent years evidence has accumulated suggesting that sleep and sleep stages might not congruently take place in the whole brain, but can also locally occur restricted to specific networks and regions [8]. For example, in human neocortex, local activations were recorded while SWS was simultaneously present in other regions [9]. In mice, intrusions of sleep-like activity patterns were observed in local neocortical networks during prolonged wake periods and immediately after spontaneous awakening [10, 11]. In simultaneous scalp and intracranial recordings in human patients, most slow waves and spindles hallmarking the EEG during SWS were found to occur only in local neocortical networks [12].

The findings of these studies mostly examine activity within neocortical networks, underlining the local nature of phenomena defining sleep stages like spindles and slow waves. However, much less is known about the congruence in the occurrence of entire sleep stages between different brain structures. This is important, on the one hand, because the different sleep stages are often thought to fulfill specific functions. For example, “dual process theories” of memory formation during sleep assume that SWS supports consolidation of declarative memory, whereas REM sleep supports consolidation of procedural memory [13, 14]. On the other hand, the functions allocated to the different sleep stages are typically not established within only a single structure such as the neocortex, but rely on interactions between cortical and subcortical interactions. Thus, memory formation during SWS is assumed to involve the co-ordinate dialogue between neocortex and hippocampus [15, 16]. Indeed, consistent with a region-specific organization of sleep stages, intracranial recordings in human patients revealed that spindles occur in the hippocampus several minutes before sleep onset [17]. In a recent first systematic examination of sleep stages in the rat neocortex and hippocampus, both regions were found to concurrently be in different sleep stages nearly as often as they were in the same [18]. In light of the strong implications of these findings for the understanding of sleep and its functions, we here sought to confirm and extend those previous experiments. In rats, we recorded the EEG via skull electrodes over the frontal and parietal cortex and, additionally, local field potentials (LFPs) from medial prefrontal cortex (mPFC) and dorsal hippocampus (dHC). Our results reveal a high congruence in the occurrence of SWS at the different recording sites, which was decreased with regard to REM sleep. In many cases, the hippocampus appeared to enter REM sleep, together with a decrease in muscle tone, substantially earlier compared with the other recording sites.

Materials and Methods

Animals

The recordings were performed in five male Long Evans rats (Janvier, Le Genest-Saint-Isle, France, 280–340 g, 14–18 weeks old). Animals were kept on a 12 hr/12 hr light/dark cycle with lights off at 19:00 hr. Water and food were available ad libitum. All experimental procedures were approved by the University of Tübingen and the local institutions in charge of animal welfare (Regierungspräsidium Tübingen).

Surgery

Standard surgical procedures were followed as described previously [19]. Animals were anesthetized with an intraperitoneal injection of fentanyl (0.005 mg/kg of body weight), midazolam (2.0 mg/kg), and medetomidin (0.15 mg/kg). They were placed into a stereotaxic frame and were supplemented with isoflurane (0.5%) if necessary. The scalp was exposed and five holes were drilled into the skull. Three EEG screw electrodes were implanted: one frontal electrode (AP: +2.6 mm, ML: −1.5 mm, with reference to Bregma), one parietal electrode (AP: −2.0 mm, ML: −2.5 mm), and one occipital reference electrode (AP: −10.0 mm, ML: 0.0 mm). Additionally, two platinum electrodes were implanted to record LFP signals: one into the right mPFC (AP: +3.0 mm, ML: +0.5 mm, DV: −3.6 mm) and one into the right dHC (AP: −3.1 mm, ML: +3.0 mm, DV: −3.6 mm). Electrode positions were confirmed by histological analysis. One stainless steel wire electrode was implanted in the neck muscle for EMG recordings. Electrodes were connected to a six-channel electrode pedestal (PlasticsOne, USA) and fixed with cold polymerizing dental resin and the wound was sutured. Rats had at least 5 days for recovery.

Electrophysiological recordings

Rats were habituated to the recording box (dark grey PVC, 30 × 30 cm, 40 cm high) for 2 days, 12 hr per day, before actual recordings started.

Experimental recordings were performed for 12 hr during the light phase, starting at 7:00 hr. The rat's behavior was simultaneously tracked using a video camera mounted on the recording box. EEG, LFP, and EMG signals were continuously recorded and digitalized using a CED Power 1401 converter and Spike2 software (Cambridge Electronic Design, UK). During the recordings, the electrodes were connected through a swiveling commutator to an amplifier (Model 15A54, Grass Technologies, USA). The screw electrode in the occipital skull served as reference for all EEG, LFP, and EMG recordings. Filtering was for the EEG between 0.1 and 300 Hz, for LFP signals a high-pass filter of 0.1 Hz was applied, and for the EMG between 30 and 300 Hz. Signals were sampled at 1 kHz.

Histology

After the last recording session, electrolytic lesions were made at the tip of the electrodes to verify their precise location (dHC and mPFC). Rats were deeply anesthetized with a lethal dose of fentanyl, midazolam, and medetomidin and intracardially perfused with saline (0.9%, wt/vol) followed by a 4 per cent paraformaldehyde fixative solution. After extraction from the skull, brains were post-fixed in 4 per cent paraformaldehyde fixative solution for 1 day. Brains were then sliced into coronal sections (70 µm) and stained with 0.5 per cent toluidine blue (Figure 1).

Figure 1.

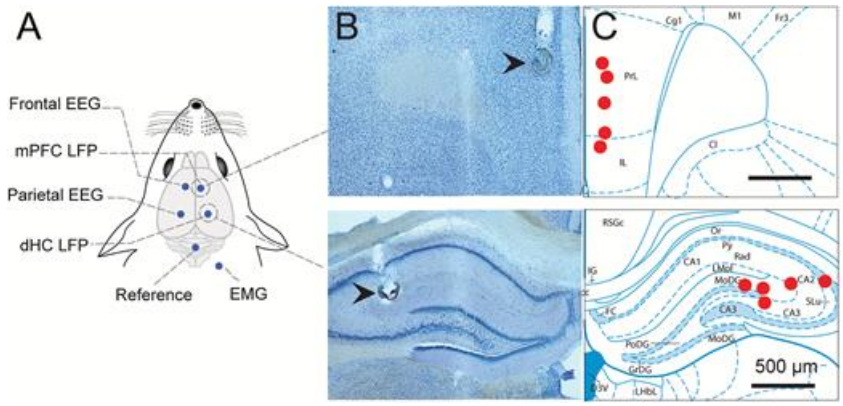

View large Download slide

Electrode positions. (A) Schema of recordings. For EEG recordings, two skull electrodes were placed above the frontal and parietal lobe, respectively, of the left hemisphere; for LFP recordings, electrodes were inserted in the mPFC and dHC, respectively, in the right hemisphere. An EMG electrode was implanted into the neck muscle. The reference for EEG, LFP, and EMG recordings was a screw electrode placed above the occipital lobe. (B) Coronal histological sections showing electrode implantation sites (arrows) in the mPFC (left top) and dHC (left bottom). (C) Maps of electrode positions for mPFC (top) and dHC (bottom) LFP recordings (3.0 and −3.22 mm anteroposterior referenced to Bregma, respectively) across five animals. EEG = Electroencephalogram; LFP = Local field potential; EMG = Electromyogram; mPFC = Medial prefrontal cortex; dHC = Dorsal hippocampus.

Sleep stage characterization

The sleep stages (SWS, IS, and REM sleep) and wakefulness were determined offline for subsequent 10 s epochs through visual inspection. For classification of sleep stages, standard criteria were followed as described by Neckelmann et al. [2] and Bjorvatn et al. [20]. Accordingly, the wake stage was characterized by predominant low-amplitude fast activity associated with increased EMG tonus. SWS was characterized by predominant high-amplitude delta activity (<4.0 Hz) and reduced EMG activity, and REM sleep by predominant theta activity (5.0–10.0 Hz), phasic muscle twitches, and minimum EMG activity. IS was identified by a decrease in delta activity, a progressive increase of theta activity and the presence of sleep spindles (10–16 Hz). Sleep stage classification was independently performed for the frontal and parietal EEG signals and the mPFC and dHC LFP signals. Each single EEG and LFP record was independently classified (together with the associated EMG record) by two experienced experimenters (interscorer agreement > 89.9%). Consensus was achieved afterwards for epochs with discrepant classification. In addition to the classical scoring based on subsequent 10 s intervals, we rescored recordings using 2 s intervals, to examine dissociations of sleep stages at a finer temporal resolution. Analyses based on the scoring of 2 s intervals confirmed essential all results of the classical 10 s scoring and will not be reported here in detail.

Data analyses

Time spent asleep and in the different sleep stages, number of episodes, and average duration of an episode in each sleep stage was calculated for

the whole 12 hr recording period. Also, for each sleep stage, the co-occurrence between any two recording sites was calculated by determining the percentage of 10 s epochs with co-occurrence of the specific sleep stage with the number of epochs with occurrence of this sleep stage in at least one of the recordings set to 100 per cent. This report is limited to the congruence between the frontal EEG signal which we used as reference (as it is most commonly used in rodent sleep research) and the three other recording sites.

To examine whether the timing of transitions into or out of specific sleep stages systematically differed between recording sites, we calculated average "delay times" for each recording site. For this purpose, the signal at the four recording sites was scanned, and whenever a transition into the sleep stage of interest occurred at one site, this time point was set to zero. Then, the transition delays for all the remaining channels were calculated based on the difference relative to this reference time point. For each recording site, the delay times to enter a specific sleep stage were averaged across all transitions into this sleep stage.

To characterize sleep stage transitions, power spectra were calculated based on MATLAB (Mathworks, USA) algorithms and the FieldTrip toolbox [21]. To this end, fast Fourier transformation (FFT) was applied to Hanning tapered blocks of 10,000 data points (corresponding to 10 s epochs), to calculate the single-sided amplitude spectrum within 0.1–25 Hz, before and after the onset of a sleep stage of interest. Power values were also used to generate time-frequency plots. Phase coherence between the dHC signal and the signal in each of the three other channels was calculated based on the frequency domain of each signal's Fourier representation computed with FieldTrip (ft_freqanalysis). To calculate EMG amplitude, the signal was root mean squared (rms), then filtered using a third-order low pass Butterworth filter of 0.2 Hz, and down-sampled to a rate of 100 Hz.

Statistical analyses

Kolmogorov–Smirnov test was used to assure normality of the distribution for each parameter. Differences in sleep stage classifications between recording sites were assessed using repeated measures analyses of variance (ANOVA) with a recording Site factor (frontal EEG, mPFC LFP, parietal EEG, dHC LFP) which was followed by post hoc paired sample *t*-tests, to specify significant differences between any two of the recording sites. For comparisons of mean power spectra, mean coherence, and mean EMG rms amplitude measures over time, nonparametric permutation tests were used with 2000 iterations [22]. A p-value of <0.05 was considered significant.

Results

Characterization of sleep stages from skull EEG and cortical and hippocampal LFP recordings

Sleep architecture was determined using the frontal EEG and EMG recordings. During the 12 hr recording period, the rats spent (mean ± SEM) 262.4 ± 14.0 min (corresponding to 36.3 ± 5.0% of the recording time) awake and 458.7 ± 13.8 min (63.7 ± 1.9%) asleep, with 364.1 ± 14.0 min (50.5 ± 5.0%) spent in SWS, 15.6 ± 2.1 min (2.2 ± 0.3%) in IS, and 79.0 ± 3.3 min (11.0 ± 0.5%) in REM sleep (Table 1). Figure 2A shows example recordings from the different recording sites for one animal. We took the frontal EEG signal as reference and determined the congruence (i.e. co-occurrence) of sleep stages between the frontal EEG and each of the three other recording sites (i.e. the parietal EEG and the LFP signals from mPFC and dHC). The congruence in wake and sleep stage occurrence during the total 12 hr period was high for time in wake (>92.0%) and SWS (>96.5%), somewhat lower for REM sleep (>87.0%), and distinctly lower for IS (<36.5%) where congruence was lowest for the mPFC LFP recordings (2.5 ± 1.6%, Figure 2B).

Table 1.

Sleep architecture during the 12 hr recording period based on the frontal EEG recordings

Sleep architecture during the 12 hr recording				
Stage	**Latency (min)**	**No. of episodes**	**Time in min**	**Time in %**
Wake	0 ± 0	161.4 ± 15.1	262.4 ± 14.0	36.4 ± 5.0
SWS	34.7 ± 4.8	172.6 ± 15.0	364.1 ± 14.0	50.5 ± 5.0
IS	118.1 ± 18.6	49.8 ± 5.1	15.6 ± 2.1	2.2 ± 0.3
REM sleep	120.0 ± 17.0	47.8 ± 5.0	79.0 ± 3.3	11.0 ± 0.5

Latency is given with reference to start of the recording period. Average time spent in the different sleep stages is given in minutes and per cent of total 12 hr recording time. $n = 5$.

SWS = Slow-wave sleep; IS = Intermediate stage; REM = Rapid eye movement.

View Large

Figure 2.

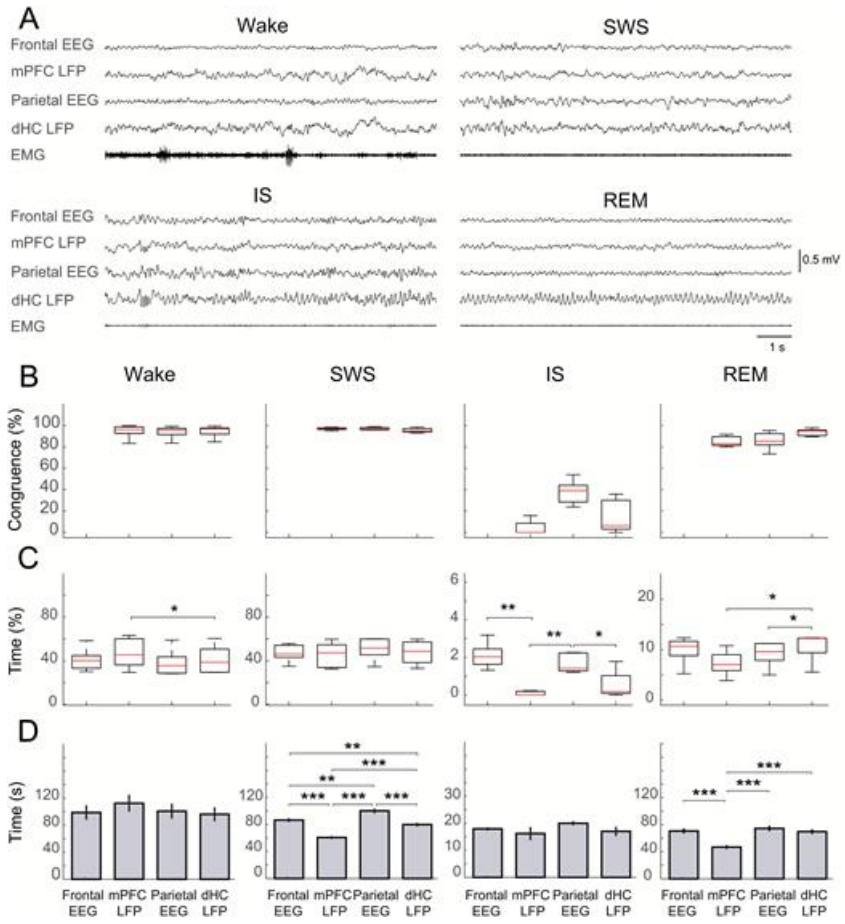

View large Download slide

Sleep stage characterization in EEG and LFP recordings. (A) Examples of 10 s epoch recordings of (from top to bottom) frontal EEG, mPFC LFP, parietal EEG, and dHC LFP during wakefulness (top left), SWS (top right), IS (bottom left), and REM sleep (bottom right). (B) Comparison of sleep stage occurrence in the different recordings. Occurrence of sleep stages in mPFC LFP, parietal EEG, and dHC LFP signals is expressed as percentage of congruence with the occurrence of the sleep stages in the frontal EEG signal used as reference. (C) Distribution of time spent awake, in SWS, IS and REM sleep and (D) average duration of episodes awake, in SWS, IS, and REM sleep for the different recording sites. Box-whisker plots indicating median, upper quartile and lower quartile, top and bottom of the box, respectively. *$p < 0.05$; **$p < 0.01$; ***$p < 0.001$ for pairwise comparison. EEG = Electroencephalogram; LFP = Local field potential; EMG = Electromyogram; mPFC = Medial prefrontal cortex; dHC = Dorsal hippocampus; SWS = Slow-wave sleep; REM = Rapid eye movement; IS = Intermediate stage.

The time spent awake and in the different sleep stages for each of the recording sites was then subjected to ANOVA which revealed significant

differences among the recording sites for time awake ($F(3, 12) = 4.02$, $p = 0.034$), time in IS ($F(3, 12) = 11.95$, $p = 0.001$), and in REM sleep ($F(3, 12) = 5.66$, $p = 0.012$), whereas time in SWS did not differ among recording sites ($F(3, 12) = 2.26$, $p = 0.134$; Figure 2C). Post hoc analyses of wake time indicated slightly longer wake times in mPFC than dHC LFP recordings ($t(4) = 2.91$, $p = 0.044$). Time in IS was longer in both frontal and parietal EEG signals compared with both mPFC and dHC LFP signals ($t \geq 5.8$, $p \leq 0.05$, for all comparisons, Figure 2C). IS was not detectable in mPFC recordings in three animals, and in dHC recordings in one animal. Time spent in REM sleep was longer in dHC than in mPFC LFP recordings, and also longer than in parietal EEG recordings ($t \geq 2.96$, $p \leq 0.041$, for all comparisons).

There were also distinct differences between the recording sites in the average duration of SWS periods ($F(2.81, 2930.4) = 60.2$, $p < 0.001$) and REM sleep periods ($F(3, 759) = 14.1$, $p < 0.001$, Figure 2D). SWS periods were generally longer in the EEG than LFP signals, and shortest in the mPFC LFP signal ($t \geq 13.3$, $p \leq 0.03$, for respective comparisons). REM sleep duration was also shortest in the mPFC signal ($t \geq 4.9$, $p \leq 0.001$, for all comparisons).

Wake–sleep transitions

Generally, the disparate appearance of sleep stages at the different recording sites concentrated on periods of transition between sleep stages. To examine whether the timing of wake-to-sleep transitions depended on the recording site, we analyzed in which of the four recording sites an ongoing wake epoch ended first (set to t = 0), and determined for each of the remaining recording sites the time interval it took to also finish the wake period and to enter sleep. The main result of this analysis was that the frontal EEG transited from wake into sleep significantly earlier than all other recording sites ($F(2.629, 1614.2) = 27.64$, $p < 0.001$, for ANOVA Site main effect, $t \geq 7.14$, $p \leq 0.001$ for respective pairwise comparisons, Figure 3A). However, although significant, the time differences were overall moderate (on average < 3.5 s) and below the 10 s resolution of visual sleep stage scoring. A corresponding analysis for sleep-to-wake transitions revealed that the frontal EEG was also the first to transit from sleep into wakefulness with this effect reaching significance for the comparisons with the mPFC LFP and parietal EEG signals ($F(3, 2022) = 9.09$, $p < 0.001$, for Site main effect, $t \geq 4.34$, $p \leq 0.001$, for pairwise comparisons).

Figure 3.

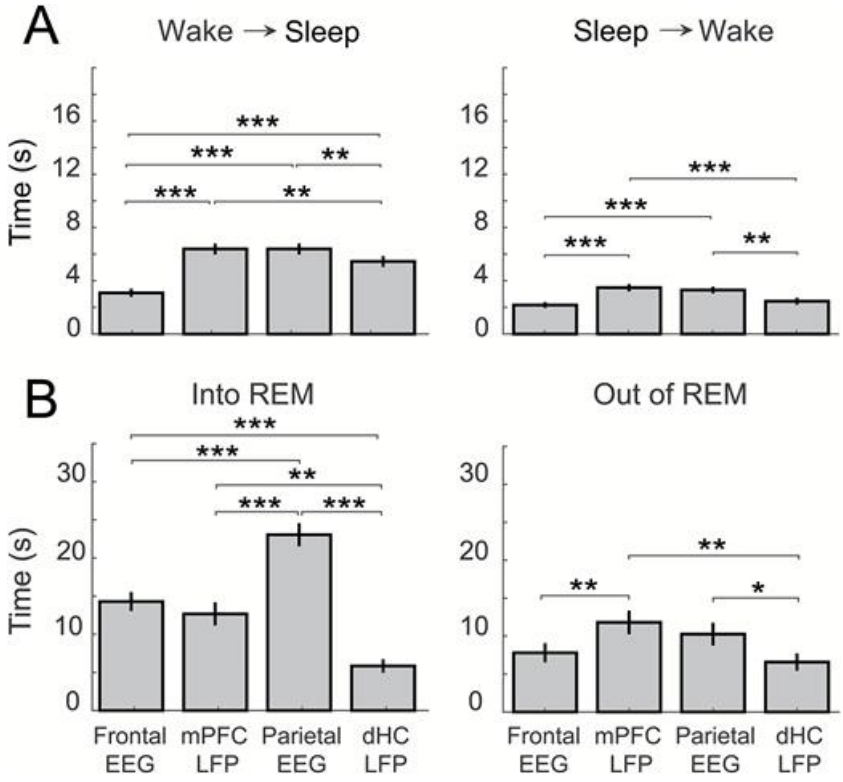

View large Download slide

Transitions into and out of sleep and REM sleep. Timing of (A) wake-to-sleep (left) and sleep-to-wake transitions (right) and (B) of transitions into REM sleep (left) and out of REM sleep (right) at the different recording sites (frontal EEG, mPFC LFP, parietal EEG and dHC LFP). In these analyses, the earliest transitions into the specified brain state occurring at a certain recording site were set to 0 s and, then, the delay time was calculated till this transition occurred at each of the other recording sites. The y-axes indicate the mean (±SEM) delay time (across all detected transitions) for each recording site. Note, overall short delay times for wake-to-sleep transitions with the frontal EEG indicating first signs of sleep following a wake period. Note also that in dHC LFP recordings REM sleep is entered

substantially earlier than at all other recording sites. **$p < 0.05$; **$p < 0.01$; ***$p < 0.001$ for pairwise comparisons. EEG = Electroencephalogram; LFP = Local field potential; mPFC = Medial prefrontal cortex; dHC = Dorsal hippocampus; REM = Rapid eye movement.

Appearance of IS and REM sleep

IS episodes were overall rather short (0.31 ± 0.04 min) and most often identified in the frontal EEG recordings (Figure 2C). IS preceded REM sleep epochs in 71.9 ± 5.1% (frontal EEG), 3.45 ± 2.18% (mPFC LFP), 61.7 ± 7.5% (parietal EEG), and 18.6 ± 11.8% (dHC LFP) of all REM sleep epochs. We determined for the periods when the frontal EEG indicated IS, the occurrence of SWS and REM sleep at the other recording sites. During these periods (with the frontal EEG indicating IS), at the other recording sites, overall more SWS than REM sleep occurred, with no significant difference in SWS percentage among the recording sites ($p > 0.75$, for Site main effect, Figure 4B). On the other hand, the percentage of REM sleep during these periods was highest in the dHC recordings, and significantly higher when compared with the mPFC LFP and parietal EEG ($F(2, 8) = 10.20$, $p = 0.006$, for Site main effect, $t \geq 4.35$, $p \leq 0.012$ for respective pairwise comparisons).

Figure 4.

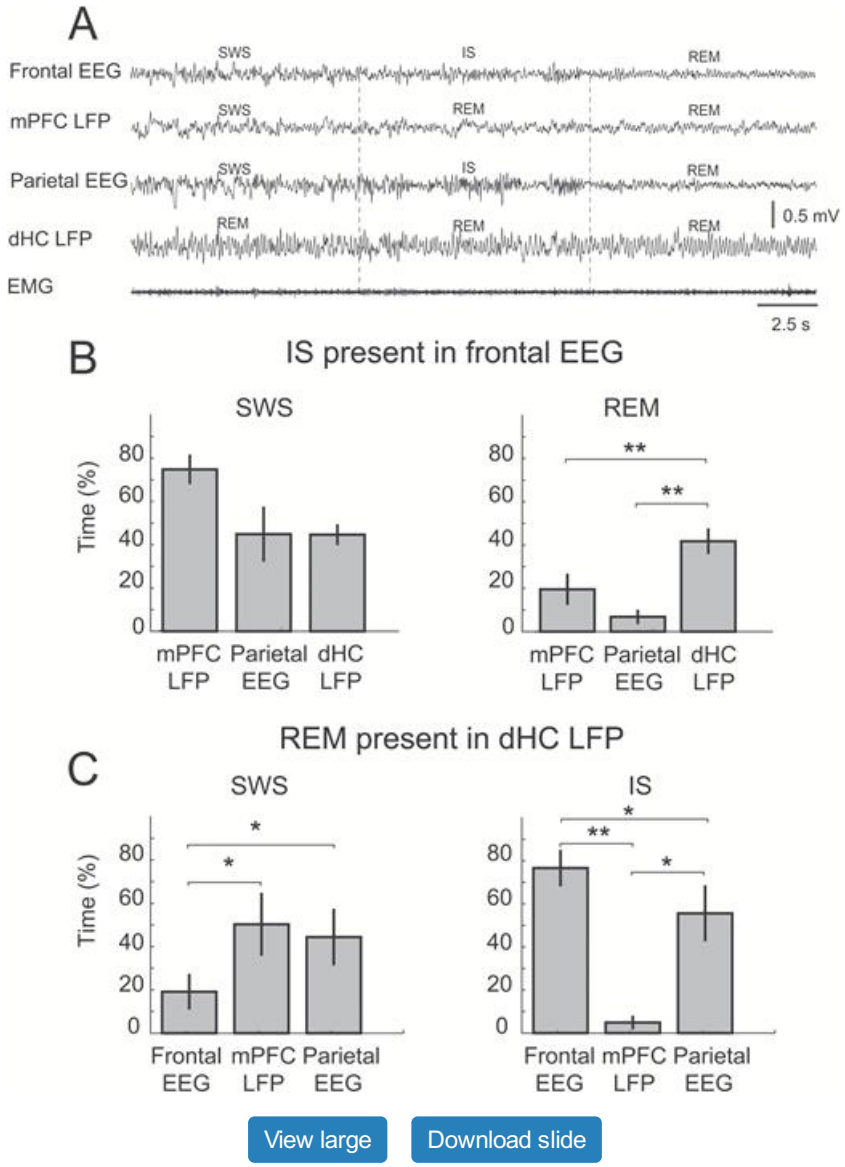

View large Download slide

Appearance of REM sleep. (A) Example recordings of frontal EEG, mPFC LFP, parietal EEG, dHC LFP, and EMG signals over three consecutive 10 s intervals. Note, while REM sleep (as identified by high theta activity) is present in dHC LFP recordings already in the first 10 s interval, at the other sites consolidated REM sleep is reached not until the third 10 s interval. EMG activity decreases already during the first 10 s interval. (B) Percentages of SWS (left) and REM sleep (right) at the different recording sites, for intervals of IS in the frontal EEG. (C) Percentages of SWS (left) and IS (right) at the different recording sites, when REM sleep had started already in dHC LFP recordings. Means (±SEM) across all epochs are indicated. *$p < 0.05$; **$p < 0.01$ for pairwise comparison. EEG = Electroencephalogram; LFP = Local field potential; EMG = Electromyogram; mPFC = Medial prefrontal cortex; dHC = Dorsal hippocampus; SWS = Slow-wave sleep; REM = Rapid eye movement; IS = Intermediate stage.

To directly examine sleep stage dynamics at the transition into REM sleep, we identified REM sleep onsets in any of the four recording sites and assessed how long it took in the respective three other recording sites to enter REM sleep (Figure 3B). This analysis revealed that REM sleep started overall substantially earlier in the dHC recordings compared with all other recording sites, with the greatest difference between REM sleep occurrence in dHC and parietal EEG recordings where REM sleep occurred with an average delay of 17.2 ± 1.1 s (with reference to dHC REM onset; $F(2.53, 387.2) = 38.21$, $p < 0.001$, for ANOVA Site main effect, $t \geq 4.23$, $p \leq 0.001$, for all pairwise comparison with dHC recordings, see Supplementary Figure S2 for results from an analysis based on the more fine-grained scoring of 2 s epochs). In 36.6 per cent of all REM sleep episodes detected (53 cases of 145), REM sleep onset in dHC recordings preceded that at all other sites (whereas in only eight cases REM sleep started simultaneously at all sites) and in 16.5 per cent of all REM sleep episodes detected (24 cases of 145), REM sleep in the dHC LFP started later than in one of the other sites. In addition, REM sleep occurred significantly earlier (by on average 8.8 ± 1.3 s) in the frontal than in the parietal EEG ($t(153) = 6.81$, $p < 0.001$). A corresponding analysis of transitions out of REM sleep revealed that REM sleep, on average also ended earliest in dHC LFP recordings. Although the respective time difference was rather small (on average < 5 s), the effect reached significance in comparison with the mPFC LFP and parietal EEG signal ($F(2.74, 421.7) = 4.29$, $p = 0.007$, for Site main effect, $t \geq 2.05$, $p \leq 0.042$, for respective pairwise comparisons Figure 3B).

We further analyzed the sleep stages in the other recordings sites when REM sleep had started first in dHC recordings. The frontal EEG indicated IS during almost 80 per cent of this time, whereas the LFP from mPFC indicated SWS most of the time, and in the parietal EEG IS and SWS each covered about half of the time (see Figure 4C also for pairwise statistical comparisons). Finally, we examined the time course of the dissociation between REM sleep onset in cortical EEG and dHC LFP recordings across the 12 hr recording period (summarized in Supplementary Figure S1). These analyses revealed that the number of REM epochs increased across this period. However, the number of REM sleep epochs with an earlier onset in dHC LFP than cortical EEG recordings remained constant and, accordingly, the proportion of such epochs with an earlier onset in hippocampal LFP recordings decreased across this time ($H(2) = 6.36$, $p = 0.042$, for Kruskal–Wallis one-way ANOVA effect of time).

Theta activity and muscle atonia at early hippocampal REM sleep onsets

We further examined those transitions into REM sleep ($n = 53$) which occurred earlier in dHC LFP recordings than at the other recordings sites. For these cases, we calculated average power spectra for EEG and LFP signals, for 10 s intervals before and after REM sleep onset, respectively. Averaging was done either time-locked to REM onset as identified in the dHC LFP recordings or time-locked to REM onset as identified in each of the respective other three recording sites (Figure 5A–C). Comparing these two ways of time-locking revealed distinct differences for the frontal and parietal EEG, i.e. power was higher in a broad frequency range including delta (1.0–4.0 Hz) and spindle (10–16 Hz) frequencies before and (though less consistently) also after the REM onsets when these REM onsets were determined in the respective EEG recordings in comparison to the spectra aligned to REM onset as defined in dHC LFP recordings. Notably this increase spared the 5.0–10.0 Hz theta band. Moreover, analyzing the coherence between recordings for cases where dHC LFP entered REM sleep first in the same way revealed a significantly reduced coherence in theta activity, particular between the dHC LFP and frontal EEG, when recordings were time-locked to the REM onset in the dHC recording (Figure 5D). Together these findings suggest that during the intervals of early local REM sleep in dHC recordings, there is also high theta activity in the cortical EEG activity that is synchronized to the hippocampal theta. However, the detection of REM sleep in the EEG signal is hampered by strong concurring SWS-related oscillatory activity.

Figure 5.

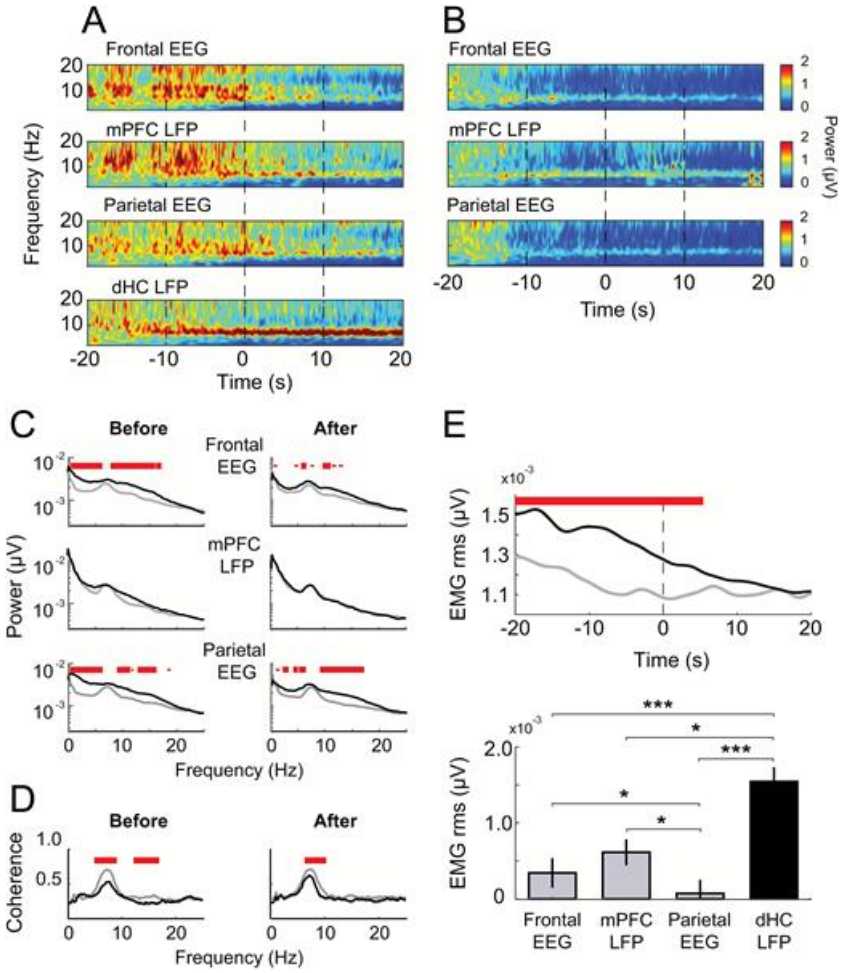

View large Download slide

Early transitions into REM sleep at dHC LFP recordings. (A, B) Average time-frequency plots (power—color coded) in the different frequency bands for frontal EEG, mPFC LFP, parietal EEG, and dHC LFP signals, during a ±20 s interval around REM sleep onset ("0 s") for the cases when REM sleep started first in dHC LFP recordings (n = 53). Averages in (A) are time-locked to REM onset as identified in dHC LFP recordings, and in (B) to REM onset as identified in each of the other three recordings sites. (C) Power spectra for 10 s epochs before (left) and after (right) REM sleep onset for the cases when REM sleep started first in dHC LFP recordings, time-locked to REM onset as identified in dHC LFP recordings (black lines), and time-locked to REM onset as identified in each of the respective other three sites (frontal EEG, mPFC LFP, and parietal EEG; grey lines). (D) Coherence between the dHC LFP signal and the frontal EEG for 10-s epochs before (left) and after (right) REM sleep onset for the cases when REM sleep started first in dHC LFP recordings, time-locked to REM onset as identified in dHC LFP recordings (black line) and time-locked to REM onset as identified in the frontal EEG (grey). (E) Upper panel: Average EMG root mean square signal during a ±20 s interval around REM sleep onset ("0 s") for the cases when REM sleep started first in dHC LFP recordings (n = 53). Averages were either time-locked to the REM sleep onset as determined in dHC LFP recordings (black solid line) or to the REM sleep onset as determined in the parietal EEG (grey line). (C, D, and E) Significant differences in power, coherence, and EMG rms, respectively, are indicated by horizontal thin ($p < 0.05$) and thick ($p < 0.01$) red lines. Bar graph below shows mean differences in EMG rms activity between the 10 s intervals before minus after REM sleep onset for these cases, with REM sleep onset determined either in frontal EEG, mPFC LFP, parietal EEG, or dHC LFP recordings. Note, highest value, i.e. strongest decrease in EMG activity for defining REM sleep onset with reference to dHC LFP signal (black bar). *$p < 0.05$; ***$p < 0.001$ for pairwise comparisons. EEG = Electroencephalogram; LFP = Local field potential; EMG = Electromyogram; mPFC = Medial prefrontal cortex; dHC = Dorsal hippocampus; rms = root mean square.

For the cases where REM sleep onset in dHC recordings preceded REM onset in the three other recording sites, we also assessed the time course of muscle atonia as another hallmark of REM sleep. Generally, root mean square (rms) EMG activity, as expected, distinctly decreased from the 10 s interval before REM sleep onset to the 10 s interval after REM sleep onset. In the cases with an earlier REM sleep onset in dHC recordings, this decrease from before to after REM sleep onset was significantly higher when the rms EMG signal was time-locked to the onset as determined in the dHC recordings, compared with time-locking the signal to REM sleep onset as determined in any of the other recording sites ($F(2.2, 84) = 9.74$, $p < 0.001$, for Site main effect, $t \geq 6.6$, $p \leq 0.03$ for pairwise comparisons, Figure 5E). Thus, earlier REM onsets in dHC recordings were also accompanied by earlier muscle atonia. A complementary analysis on the cases where REM sleep occurred in dHC LFP recordings occurred later than at least one of the other three recording sites, did reveal hints that in these cases atonia is specifically coupled to REM occurrence in the

hippocampal recording (Supplementary Figure S3).

Discussion

We compared in rats the expression of sleep stages in EEG recordings over frontal and parietal cortex and in LFP recordings from mPFC and dHC, and found distinct differences between cortical and hippocampal signals that mainly pertained to the timing of REM sleep. In dHC LFP recordings, REM sleep epochs in many cases started substantially earlier than at the other recording sites preferentially covering neocortical activity, which confirms recent findings by Emrick et al. [18]. The early start of REM sleep in hippocampal recordings, moreover, was accompanied by a REM sleep-typical decrease in muscle tone. We also found differences in the occurrence of SWS at the different recording sites. However, compared with those found for REM sleep, these were overall marginal. In fact, determination of SWS in neocortical and hippocampal signals was hallmarked by a very high congruence of greater than 95 per cent. Our findings underline that differences in the regional expression of sleep stages need to be considered when it comes to characterizing the function of sleep stages, especially of REM sleep.

The high congruence of SWS at the different recording sites with no differences in the time spent in SWS in neocortical and hippocampal signals suggests that SWS reflects a rather unitary phenomenon that catches widespread areas of the brain. Classification of SWS relies mainly on the occurrence of slow waves including the <1.0 Hz slow oscillation. These oscillations are generated in thalamo-cortical networks [23–26]. Beyond synchronizing activity in these regions, the oscillations are also known to synchronize activity in several other brain regions including the hippocampus, thereby allowing precisely timed interactions between these regions [19, 27–29]. However, despite the high congruence in the occurrence of SWS at the different sites, there were subtle differences. At a first glance, it appears surprising that in the mPFC LFP signal the mean duration of SWS epochs was on average slightly shorter than at the other sites, because the prefrontal cortex is thought to be a major source of slow waves [30]. However, an LFP recording from deep layers of the mPFC is expected to be most sensitive to and to pick up only locally generated slow potential changes, whereas the amplitude of slow wave potentials originating from other sites is comparatively low at this site. By contrast, skull EEG electrodes, although receiving an overall diminished potential, pick up slow-wave signals from rather broad cortical areas. Consistent with this explanation, we found that the prefrontal EEG signal was the first to indicate the occurrence of SWS. Again, it is to emphasize that these differences were marginal and appear to mainly reflect the different sensitivity of LFP and EEG recordings to the slow-wave signal.

Contrasting with the SWS-related findings, the observed differences in REM sleep occurrence appeared to reflect a disparate regulation of this sleep stage in neocortical and hippocampal networks, which were most obvious at the transition into this sleep stage. This was evident already in the analyses of IS which in rats is defined as a transition stage between SWS and REM sleep, mainly characterized by the simultaneous occurrence of spindle-like activity and theta activity. Apart from the fact that co-occurrence of IS at the different sites was quite low (<37%), we found that IS epochs mainly occurred in EEG recordings covering frontal cortical signal, and that while the frontal cortex was in IS, the hippocampal LFP signaled already the presence of REM sleep much more often than the other recording sites (Figure 4B). Conversely, during early REM sleep onsets in hippocampal LFP recordings, the frontal EEG signaled the presence of IS in almost 80 per cent of the cases (Figure 4C), altogether suggesting that the spread of hippocampal theta activity might contribute to classification of IS in the cortical signal. Indeed, due to its amalgamate nature and the resulting difficulties to determine this sleep stage, in many studies IS is not considered as a separate stage from SWS.

The view of a disparate regulation REM sleep in hippocampal and neocortical networks is corroborated by our finding that REM sleep onset in hippocampal LFP recordings on average substantially preceded REM onsets at the other recoding sites. This finding confirms and extends findings from a previous study [18], which overall reported an even stronger asynchrony in the occurrence of REM sleep comparing skull EEG recordings with dorsal hippocampal LFP recordings. Of note, in that study hippocampal LFP recordings were referenced to an electrode in neocortical deep white matter, which contrasts with the present recordings employing an occipital skull electrode. Although widely used in standard LFP recordings, such reference electrode might bias hippocampal LFP recordings due to EEG activity picked up from underlying cerebellum [31]. However, comparing our present dHC LFP recordings with those in other studies using different electrode montages did not reveal obvious alterations, e.g. with regard to the occurrence of spindles and theta activity. Also, theta activity (used as core signal for the determination of REM sleep) showed up in very much the same way when, for exploratory purposes, we re-referenced the dHC LFP signal to the medial prefrontal LFP electrode. Nevertheless, although a substantial bias seems unlikely, the precise contribution of cerebellar EEG activity during sleep to the dHC LFP signal using an occipital skull reference is presently unclear. It is hence the more important that the central findings of our study quite well agree with those of Emrick et al., despite their use of a rather different reference for LFP recordings. Note, our findings exclude an independent regulation of REM sleep in the hippocampus because in the hippocampus REM sleep much more often preceded that followed the occurrence of REM sleep in neocortex. The signal hallmarking REM sleep is 5.0–10.0 Hz theta activity which, however, also occurs during (active) wakefulness [32, 33]. Generation of the theta rhythm involves the medial septum along with the diagonal band of Broca which directly projects to the hippocampus, with the hippocampal network representing the major theta current generator [33, 34]. In this way, the first appearance of REM sleep in hippocampal networks and before

the appearance in neocortex might partly be a consequence of this direct innervation of the hippocampus from theta generating structures. However, the early appearance of REM sleep in hippocampal recordings, in our study, was also coupled to a distinct decrease in muscle tone (Figure 5E), another major feature of REM sleep, with this coupling pointing to the involvement of brainstem mechanisms in the disparate regulation of hippocampal REM sleep. The meso-pontine area of the brainstem, including *REM-off* and *REM-on* networks, has been proposed as a switch between REM sleep and SWS [35]. Different populations of the *REM-on* network project to the basal forebrain (including theta generating structures of the medial septum and diagonal band of Broca) and to medullary nuclei and the spinal cord where they contribute to establishing muscle atonia [35–37]. Thus, projections of these brainstem *REM-on* networks are likely capable of mediating a concurrent increase in hippocampal theta activity and muscle atonia.

Interestingly, in the cases where REM sleep occurred earlier in hippocampal networks, our spectral analyses of the EEG signal during this interval revealed enhanced power in wide frequency ranges including the 0.5–4.0 Hz slow wave activity and the 10–16 Hz spindle activity ranges characteristic for SWS, but sparing the 5.0–10.0 Hz theta range (Figure 5C). Notably, this increase spared the 5.0–10.0 Hz theta range reflecting that the EEG recordings at that time also expressed high theta activity which—as revealed by coherence analyses—appeared to be synchronized in phase with the hippocampal theta rhythm (Figure 5D). Thus, when REM sleep occurs earlier in the hippocampus than neocortex, this appears to be due to SWS-related activity still capturing neocortical networks, in the presence of REM-related theta activity that in the EEG, at that time, probably represents volume-conducted hippocampal activity [38, 39]. This conclusion is further supported by our analysis of the time course in dissociation of cortical and hippocampal REM sleep onset, indicating enhanced proportion of REM sleep epochs with earlier onset in hippocampal networks in the beginning of the recording (light) period when sleep and pressure were high. Thus, the expression of theta activity per se in the cortical EEG during this time of local hippocampal REM sleep appears not to be hindered by the simultaneous appearance of slow wave and spindle frequency activity [40]. The mechanisms that then, with some delay, make neocortical networks to ultimately synchronize to the hippocampal theta rhythm remain to be clarified.

In sum, our data are consistent with the concept that sleep and SWS for the most part present as global phenomena with a common impact on different brain regions. However, the occurrence of REM sleep underlies region-specific regulatory mechanisms, in as much this sleep stage in many cases begins substantially earlier in hippocampal than neocortical networks. Future studies need to characterize the mechanisms mediating this dissociation between hippocampal and neocortical networks, and the question to what extent this dissociation might become stronger with increased propensity of sleep and SWS. Whatever the case, the present findings might be also of relevance for the understanding of the functions (like memory formation) that have been associated with the stage of REM sleep and involve respective structures of interest [41, 42].

Supplementary Material

Supplementary material is available at *SLEEP* online.

Funding

This work was supported by the Deutsche Forschungsgemein schaft (TR-SFB 654 Plasticity and Sleep). E.D. was supported by a VRI Scholarship from the Pontificia Universidad Católica de Chile.

Notes

Conflict of interest statement. The authors declare that the research was conducted in the absence of any commercial or financial relationships that could be construed as a potential conflict of interest.

Acknowledgments

We thank Dr. Hong-Viet Ngo and Ms. Ilona Sauter for help with data analyses and histology, respectively.

References

1. Rechtschaffen A, Kales A.*A Manual of Standardized Terminology, Techniques and Scoring System for Sleep Stages of Human Subjects* . Bethesda, MD: U. S. National Institute of Neurological Diseases and Blindness, Neurological Information Network; 1968.

2. Neckelmann Det al. The reliability and functional validity of visual and semiautomatic sleep/wake scoring in the Møll-Wistar rat. *Sleep* . 1994;17(2):120–131.
   Google Scholar Crossref PubMed

3. Tobler I. Is sleep fundamentally different between mammalian species?*Behav Brain Res* . 1995;69(1-2):35–41.
   Google Scholar Crossref PubMed

4. Lesku JAet al. A phylogenetic analysis of sleep architecture in mammals: the integration of anatomy, physiology, and ecology. *Am Nat* . 2006;168(4):441–453.
   Google Scholar Crossref PubMed

5. Gottesmann Cet al. Intermediate stage of sleep in the cat. *J Physiol (Paris)* . 1984;79(5):365–372.
   Google Scholar PubMed

6. Glin Let al. The intermediate stage of sleep in mice. *Physiol Behav* . 1991;50(5):951–953.
   Google Scholar Crossref PubMed

7. Benington JHet al. Scoring transitions to REM sleep in rats based on the EEG phenomena of pre-REM sleep: an improved analysis of sleep structure. *Sleep* . 1994;17(1):28–36.
   Google Scholar Crossref PubMed

8. Krueger JMet al. Sleep as a fundamental property of neuronal assemblies. *Nat Rev Neurosci* . 2008;9(12):910–919.
   Google Scholar Crossref PubMed

9. Nobili Let al. Dissociated wake-like and sleep-like electro-cortical activity during sleep. *Neuroimage* . 2011;58(2):612–619.
   Google Scholar Crossref PubMed

10. Vyazovskiy VVet al. Local sleep in awake rats. *Nature* . 2011;472(7344):443–447.
    Google Scholar Crossref PubMed

11. Vyazovskiy VVet al. The dynamics of cortical neuronal activity in the first minutes after spontaneous awakening in rats and mice. *Sleep* . 2014;37(8):1337–1347.
    Google Scholar Crossref PubMed

12. Nir Yet al. Regional slow waves and spindles in human sleep. *Neuron* . 2011;70(1):153–169.
    Google Scholar Crossref PubMed

13. Maquet P. The role of sleep in learning and memory. *Science* . 2001;294(5544):1048–1052.
    Google Scholar Crossref PubMed

14. Rasch Bet al. About sleep's role in memory. *Physiol Rev* . 2013;93(2):681–766.
    Google Scholar Crossref PubMed

15. Diekelmann Set al. The memory function of sleep. *Nat Rev Neurosci* . 2010;11(2):114–126.
Google Scholar PubMed

16. Watson BOet al. Sleep, memory & brain rhythms. *Daedalus* . 2015;144(1):67–82.
Google Scholar Crossref PubMed

17. Sarasso Set al. Hippocampal sleep spindles preceding neocortical sleep onset in humans. *Neuroimage* . 2014;86:425–432.
Google Scholar Crossref PubMed

18. Emrick JJet al. Different simultaneous sleep states in the hippocampus and neocortex. *Sleep* . 2016;39(12):2201–2209.
Google Scholar Crossref PubMed

19. Mölle Met al. Hippocampal sharp wave-ripples linked to slow oscillations in rat slow-wave sleep. *J Neurophysiol* . 2006;96(1):62–70.
Google Scholar Crossref PubMed

20. Bjorvatn Bet al. EEG power densities (0.5-20 Hz) in different sleep-wake stages in rats. *Physiol Behav* . 1998;63(3):413–417.
Google Scholar Crossref PubMed

21. Oostenveld Ret al. FieldTrip: open source software for advanced analysis of MEG, EEG, and invasive electrophysiological data. *Comput Intell Neurosci* . 2011;2011:156869.
Google Scholar Crossref PubMed

22. Maris Eet al. Nonparametric statistical testing of EEG- and MEG-data. *J Neurosci Methods* . 2007;164(1):177–190.
Google Scholar Crossref PubMed

23. Steriade Met al. Thalamocortical oscillations in the sleeping and aroused brain. *Science* . 1993;262(5134):679–685.
Google Scholar Crossref PubMed

24. Hughes SWet al. Cellular mechanisms of the slow (<1 Hz) oscillation in thalamocortical neurons in vitro. *Neuron* . 2002;33(6):947–958.
Google Scholar Crossref PubMed

25. Steriade M. Grouping of brain rhythms in corticothalamic systems. *Neuroscience* . 2006;137(4):1087–1106.
Google Scholar Crossref PubMed

26. Crunelli Vet al. The slow (<1 Hz) rhythm of non-REM sleep: a dialogue between three cardinal oscillators. *Nat Neurosci* . 2010;13(1):9–17.
Google Scholar Crossref PubMed

27. Siapas AGet al. Coordinated interactions between hippocampal ripples and cortical spindles during slow-wave sleep. *Neuron* . 1998;21(5):1123–1128.
Google Scholar Crossref PubMed

28. Wierzynski CMet al. State-dependent spike-timing relationships between hippocampal and prefrontal circuits during

sleep. *Neuron* . 2009;61(4):587–596.
Google Scholar Crossref PubMed

29. Maingret Net al. Hippocampo-cortical coupling mediates memory consolidation during sleep. *Nat Neurosci* . 2016;19(7):959–964.
Google Scholar Crossref PubMed

30. Riedner BAet al. Temporal dynamics of cortical sources underlying spontaneous and peripherally evoked slow waves. *Prog Brain Res* . 2011;193:201–218.
Google Scholar Crossref PubMed

31. Canto CBet al. The sleeping cerebellum. *Trends Neurosci* . 2017;40(5):309–323.
Google Scholar Crossref PubMed

32. Bland BH. The physiology and pharmacology of hippocampal formation theta rhythms. *Prog Neurobiol* . 1986;26(1):1–54.
Google Scholar Crossref PubMed

33. Buzsáki G. Theta oscillations in the hippocampus. *Neuron* . 2002;33(3):325–340.
Google Scholar Crossref PubMed

34. Pignatelli Met al. Neural circuits underlying the generation of theta oscillations. *J Physiol Paris* . 2012;106(3-4):81–92.
Google Scholar Crossref PubMed

35. Lu Jet al. A putative flip-flop switch for control of REM sleep. *Nature* . 2006;441(7093):589–594.
Google Scholar Crossref PubMed

36. Krenzer Met al. Brainstem and spinal cord circuitry regulating REM sleep and muscle atonia. *PLoS One* . 2011;6(10):e24998.
Google Scholar Crossref PubMed

37. Fraigne JJet al. REM sleep at its core – circuits, neurotransmitters, and pathophysiology. *Front Neurol* . 2015;6:1–9.
Google Scholar Crossref PubMed

38. Scheffzük Cet al. Selective coupling between theta phase and neocortical fast gamma oscillations during REM-sleep in mice. *PLoS One* . 2011;6(12):e28489.
Google Scholar Crossref PubMed

39. Scheffzük Cet al. Global slowing of network oscillations in mouse neocortex by diazepam. *Neuropharmacology* . 2013;65:123–133.
Google Scholar Crossref PubMed

40. Lecci Set al. Coordinated infraslow neural and cardiac oscillations mark fragility and offline periods in mammalian sleep. *Sci Adv* . 2017;3(2):e1602026.
Google Scholar Crossref PubMed

41. Ribeiro S. Sleep and plasticity. *Pflugers Arch* . 2012;463(1):111–120.
Google Scholar Crossref PubMed

42. Calais JBet al. Experience-dependent upregulation of multiple plasticity factors in the hippocampus during early REM sleep. *Neurobiol Learn Mem* . 2015;122:19–27.
Google Scholar Crossref PubMed

Author notes

These authors contributed equally to this work.

Shared senior authorship

Topic:

electroencephalography

hippocampus

neocortex

prefrontal cortex

cranium

sleep stages

rem sleep

sleep

sleep, slow-wave

Issue Section: Basic Science of Sleep and Circadian Rhythms

- Supplementary data

Supplementary data

Supplementary FigureS1 - png file
Supplementary FigureS2 - png file
Supplementary FigureS3 - png file
Supplemental Material - docx file

View Metrics

More on this topic

Effects of Method, Duration, and Sleep Stage on Rebounds from Sleep Deprivation in the Rat

Rapid Eye Movement and Non-Rapid Eye Movement Sleep Contributions in Memory Consolidation and Resistance to Retroactive Interference for Verbal Material

Aging Effects on Cardiac and Respiratory Dynamics in Healthy Subjects across Sleep Stages

Relationship of Epileptic Seizures to Sleep Stage and Sleep Depth

Related articles in

Web of Science

Google Scholar

Related articles in PubMed

Practical Considerations for the Academic Physician Moving to a New State.

Hybrid scattering-LSTM networks for automated detection of sleep arousals.

Postpartum fatigue, daytime sleepiness, and psychomotor vigilance are modifiable through a brief residential early parenting program.

Association between sleep duration and attention-deficit hyperactivity disorder: A systematic review and meta-analysis of observational studies[âœ°].

Citing articles via

Web of Science (1)

Google Scholar

CrossRef

Latest | **Most Read** | **Most Cited**

Characterization of the sleep disorder of anti-IgLON5 disease

Actigraphic detection of periodic limb movements: development and validation of a potential device-independent algorithm. A proof of concept study

Simultaneous tonic and phasic REM sleep without atonia best predicts early phenoconversion to neurodegenerative disease in idiopathic REM sleep behavior disorder

Residual symptoms after natural remission of insomnia: associations with relapse over 4 years

Sleep duration and fragmentation in relation to leukocyte DNA methylation in adolescents

Online ISSN 1550-9109
Print ISSN 0161-8105